Subcarrier Pairing and Power Allocation With Interference Management in Cognitive Relay Networks Based on Genetic Algorithms

Hung-Sheng Lang, Shih-Chun Lin, *Member, IEEE*, and Wen-Hsien Fang

***Abstract*—This paper considers the resource allocation for an orthogonal-frequency-division-multiplexing (OFDM)-based cognitive decode-and-forward (DF) relay network. Our objective is to maximize the sum rate (over subcarriers) of the cognitive-radio user with the interference introduced to the primary users (PUs) being managed. The optimization is over subcarrier pairing and power allocation, which leads to a mixed-integer programming (MIP) problem. To resolve this complicated MIP problem at a reasonable cost, we adopt the heterogeneous genetic algorithm (HGA) framework. The main motivation for the HGA framework comes from the idea that it can reduce the impact of extra assumptions made in previous works to simplify the problem. In our HGA, the chromosome is divided into an integer string for subcarrier pairing and a real-number string for power allocation. Two new initialization methods of these chromosomes, which are motivated by the convex optimization theory, are proposed. New crossover and mutation schemes are also devised to accommodate these new chromosomes, as well as to manage the interference to the PUs. Furthermore, we also propose a two-stage low-complexity genetic algorithm, which separately determines the proper subcarrier pairs and power allocations. Our simulations show that our HGAs and the two-stage algorithm provide competing performance, compared with similar state-of-the-art works.**

***Index Terms*—Cognitive radio, genetic algorithms, mixed integer programming, power allocation, subcarrier pairing.**

I. Introduction

EFFICIENT spectrum usage is essential to meet the increasing demand for high-data-rate services. However, measurements from the Federal Communications Commission have indicated that, for approximately 90% of the time, licensed frequency bands are unused and, hence, wasted. Due to this reason, many research efforts have been devoted to studies on the so-called cognitive radio (CR) technology [1]–[5], which enables unlicensed (or secondary) users to dynamically sense unused spectrum segments and communicate via these spectrum segments with limited interference on licensed (or primary) users. To further increase the data rates, the relay-aided communications [6], [7] are promising techniques, which allow the secondary users (SUs) to transmit their messages through the relay stations. The relay paths provide spatial diversity that can be exploited to enhance the throughputs or the outage probabilities, particularly when the link strength between the SU and the destination is weak. In the literature, many relaying strategies [6], [8]–[10], such as decode-and-forward (DF), amplify-and-forward (AF), and selective relaying, have been proposed to achieve this task.

In multipath fading channels, the relay-aided systems using orthogonal frequency-division multiplexing (OFDM) [11] are promising communication techniques for the SUs. The OFDM transmission can turn the time-domain multipath fading into an equivalent frequency-domain single-path fading and simplify the receiver design. In this paper, we focus on an OFDM-based cognitive network where an SU communicates with a destination through a DF relay, while multiple primary users (PUs) exist in the network. Together with the power allocation on each subcarrier [10], for our OFDM-based relay systems, proper subcarrier pairing [12] can further improve the SU's transmission rate while controlling the interference to the PUs. Subcarrier pairing decides, after decoding the data on a certain subcarrier for the SU–relay (S–R) link, on an appropriate subcarrier for the relay–destination (R–D) link to forward the decoded data. We will study the joint power allocation and subcarrier pairing problems for the SU and the DF relay, under the constraints that the interference to the multiple PUs must be managed.

In the literature, several works study the power allocation and/or subcarrier pairing problems, with [13], [14] or without [12], [15]–[17] the interference management constraints for the PU. First, in [12], a heuristic sorted channel-pairing scheme was proposed for subcarrier pairing, where the subcarriers for the S–R and R–D links were first sorted according to the corresponding channel gains, and then, each of the subcarriers for the S–R links was paired with that for the R–D links with the same rank. A joint optimization method was proposed in [15] by continuously relaxing the integer subcarrier pairing constraints and solving the corresponding Lagrange dual problems [19]. Parallel to the sum-rate optimization problem in [15], the work in [17] considered joint optimization for the power minimization problem. However, continuous relaxation

Manuscript received November 28, 2014; revised June 10, 2015 and August 27, 2015; accepted September 2, 2015. Date of publication September 28, 2015; date of current version September 15, 2016. This work was supported by the Ministry of Science and Technology, Taiwan, under Grant MOST 104-2221-E-011-048 and Grant MOST 104-2628-E-011-008-MY3 and by the Ministry of Education, Taiwan, under "Aiming for the Top University Program." The review of this paper was coordinated by Prof. M. C. Gursoy.

The authors are with the Department of Electronic and Computer Engineering, National Taiwan University of Science and Technology, Taipei 10607, Taiwan (e-mail: m10002234@mail.ntust.edu.tw; sclin@mail.ntust.edu.tw; whf@mail.ntust.edu.tw).

Color versions of one or more of the figures in this paper are available online at http://ieeexplore.ieee.org.

Digital Object Identifier 10.1109/TVT.2015.2483199

used in [15] and [17] may result in loss of optimality. Contrary to the aforementioned works [12], [15]–[17], the interference management constraints for the PU were considered in [13] and [14]. However, there was no relay employed in the cognitive network in [13]. Moreover, the works in [9] and [14] (also [16]) considered the sensations with AF relays. Compared with the achievable rate of the DF relay in our setting, the achievable rate of the AF relay in [9] and [14] and the resulting target function for optimization are different from ours. In [30], the joint power allocation and subcarrier pairing optimization was studied without CR constraints, but with limited channel state information feedback. In [31], similar joint optimizations without CR constraints were studied, but in the downlink channel with multiple receivers. In [18], the quality-of-service-aware relay selection and subcarrier assignment in multiuser orthogonal frequency-division multiple-access (OFDMA) relay networks was considered without CR constraints. As a whole, the settings in [12]–[18], [30], and [31] are fundamentally different from ours, where the DF relay is used, and single/multiple-carrier PUs are allowed in the cognitive network.

In contrast to [12]–[17], here, we propose a new approach based on the generic algorithm (GA) framework [20] for joint power allocation and subcarrier pairing with DF relay under interference management constraints for the PUs. The GA is an effective optimization technique that emulates the crossover and mutation phases in the evolution of a chromosome to efficaciously search for the optimal solution [20]–[22]. However, the joint power allocation and subcarrier pairing problem is mixed-integer programming (MIP), since the power is real positive numbers, whereas the subcarrier pairing is integers. As such, as opposed to the conventional GAs, where the chromosomes are composed of a single bit string, an integer string, or a real-number string [22], [23], here, we propose a *heterogeneous* generic algorithm (HGA) to solve the MIP. Now, the chromosomes are divided into an integer string for subcarrier pairing and a real-number string for power allocation. It is well known that the performance of GAs, similar to other stochastic search algorithms, heavily hinges on the judicious choices of initializations to yield good performance [22]. We, thus, propose two new initialization methods inspired by the convex optimization theory [19], [24]. Apart from the initialization, new crossover and mutation steps are implemented, tailoring for the new chromosomes as well as for interference management constraints for the PUs. The resulting HGA with either initialization method has better performance compared with the previous works. Moreover, to reduce the computational load, we also propose a lower complexity two-stage algorithm that separately solves subcarrier pairing and power allocation via GAs. Part of this paper has appeared in [25].

Our contributions are itemized as follows.

1) We use the GA framework to reduce the impact of extra assumptions made for applying convex optimization techniques. Although the convex optimization techniques were common for solving resource allocations for OFDM-based DF systems [15], [29], these works always made the assumption for subcarrier pairings [see (6)]. This assumption is imposed to simplify the target DF rate function, and thus, the convex optimization technique can be invoked. However, such an assumption is hard to meet, particularly for the systems with CR constraints. The detailed discussions are given after (8). On the contrary, the assumption (6) is only imposed in our initialization step to find the initial or baseline parent chromosomes. After the initialization, our HGA is based on the true rate function without imposing additional assumptions.
2) We replace the widespread random initializations with the convex optimization techniques in the GA to attain superior throughput. In our problems, applying the GA techniques with random initializations seriously deteriorates the throughput. Although the Lagrange-dual-function-based approach has been employed in previous works [15], [29], we further enhance the Lagrange-dual-function-based initialization (our first HGA) with the Karush–Kuhn–Tucker (KKT) residue (our second HGA). Our second HGA, which provides superior performance, yet with substantially reduced complexity compared with previous works, does not appear in the literature.
3) We utilize the HGA to simultaneously solve subcarrier pairing and power allocation in the OFDM-based DF CR systems without any relaxation and approximation. It is noteworthy that to suit the problem considered, the chromosomes employed are very different from those in the existing GAs. To the authors' best knowledge, it is the first time the chromosomes are comprised of such a combination of integer string and real-number string. A new evolution process, including the mutation and crossover steps, was also tailored to these new types of chromosomes and the systems considered.

The remainder of this paper is organized as follows. Section II introduces the system model employed and our optimization problem. Our HGA and the two-stage algorithm are addressed in Sections III and IV, respectively. In Section V, simulations are conducted to justify the proposed approaches, and in Section VI, the concluding remarks are addressed.

II. System Model and Problem Formulation

A. System Model

Consider a two-hop OFDM-based cognitive relay network, as shown in Fig. 1, which consists of one source and destination pair of the SU,[1] one relay node, and multiple source and destination pairs of the PUs. The relay is assumed to operate in the half-duplex mode with a two-phase DF protocol; hence, it listens to the signal from the SU (also the interference from the PU) in Phase I and tries to decode the corresponding message and transmits the reencoded signal in Phase II. Here, we assume that the whole spectrum used by the SU and the relay is divided

[1] In this paper, we consider the OFDM system where multiple subcarriers are used for the SU. For the OFDMA system where there are multiple CR transmission pairs, our formulation also applies to optimize the sum rate over all SUs when each SU is allowed to choose all subcarriers in the system. Note that our sum rate is summed up over all subcarriers (and, thus, all users in the OFDMA system). However, if each SU is only allowed to choose a certain group of subcarriers, then additional constraints and variables will be needed (for identifying the grouping of subcarriers). This extension is beyond the scope of our paper.

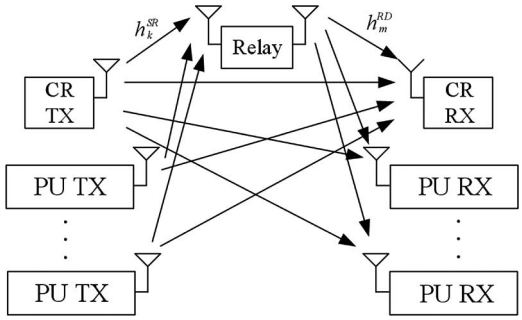

Fig. 1. Cognitive relay network model. Here, TX and RX are abbreviations for transmitter and receiver, respectively.

by Z_S subcarriers. After correctly decoding the message of the kth subcarrier (subcarrier with index k) of the SU in Phase I, the relay has the flexibility to choose a proper m subcarrier (subcarrier with index m) to transmit the reencoded signal, where $k, m \in \{1, \ldots, Z_S\}$. The (k, m) is then referred to as a subcarrier pair [15]. For such a pair (k, m), in Phase I, the received signal y_k^R at the relay on subcarrier k is expressed as

$$y_k^R = \sqrt{p_k^S} h_k^{SR} s_k + J_k^{PR} + n_k^R, \quad k = 1, \ldots, Z_S \tag{1}$$

where, for subcarrier k, p_k^S is the power of the SU's normalized signal s_k with $E[|s_k|^2] = 1$, h_k^{SR} is the complex channel coefficient from the SU to the relay, J_k^{PR} is the interference introduced by the PU to the relay, and n_k^R is the complex additive white Gaussian noise with zero mean and variance N_0. Here, $E[\cdot]$ denotes the expectation operation. In Phase II, for subcarrier pair (k, m), the signal received by the destination on subcarrier m can be written as

$$y_m^D = \sqrt{p_m^R} h_m^{RD} r_k + J_m^{PD} + n_m^D, \quad m = 1, \ldots, Z_S \tag{2}$$

where, for subcarrier m, p_m^R is the power of the relay's normalized reencoded signal r_k with $E[|r_k|^2] = 1$, h_m^{RD} is the channel coefficient from the relay to the destination, J_m^{PD} is the interference introduced by the PU to the destination, and n_m^D is the Gaussian noise with zero mean and variance N_0. We assume that the relay uses the same codebook as the SU, and to ensure that the decoding will be successful at subcarrier k at the relay and at subcarrier m at the destination, the allocated rate $R_{k,m}$ must meet the following constraint [15] for the aforementioned DF protocol:

$$R_{k,m} \le \min\left\{\log\left(1 + H_k^{SR} p_k^S\right), \log(1 + H_m^{RD} p_m^R)\right\} \tag{3}$$

where, from y_k^R in (1) and y_m^D in (2), $H_k^{SR} = |h_k^{SR}|^2/(N_0 + J_k^{PR})$ and $H_m^{RD} = |h_k^{RD}|^2/(N_0 + J_m^{PD})$ are the normalized channel gains at the relay and the destination, respectively.

We assume that the spectrum is shared by Z_p PUs, the SU, and the relay. The interferences introduced to the lth PU, $l = 1, \ldots, Z_P$, from the SU and the relay in Phases I and II are

$$\sum_{k=1}^{Z_S} p_k^S \Omega_k^{S,l} \quad \text{and} \quad \sum_{m=1}^{Z_S} p_m^R \Omega_m^{R,l}, \quad l = 1, \ldots, Z_P \tag{4}$$

respectively, where p_k^S is the power of the SU's kth subcarrier in (1), and $\Omega_k^{S,l}$ is the equivalent channel gain from such a subcarrier to the lth PU, whereas p_m^R and $\Omega_m^{R,l}$ are similarly defined as p_k^S and $\Omega_k^{S,l}$ but for the relay. The equivalent channel gains $\Omega_k^{S,l}$ and $\Omega_m^{R,l}$ can be easily obtained from the methods in [13]. The two interference terms in (4) must be limited within a threshold I_{th} for the SU to coexist with the PU.

B. Problem Formulation

Based on the cognitive relay network discussed in Section II-A, we aim to maximize the sum rate over all subcarrier pairs from (3) with the interference introduced to the PU in (4) being managed within a tolerable threshold. Let $t_{k,m}$ be the subcarrier pairing indicator, which is 1 if the kth subcarrier of the SU is selected with the mth subcarrier of the relay, and zero otherwise. Our arguments for the sum-rate optimization problem are $t_{k,m}$ as well as p_k^S and p_m^R, the power values transmitted over the kth and mth subcarriers from the SU and the relay, respectively. From (3), the overall optimization problem can be posted as follows:

$$\max_{p_k^S, p_m^R, t_{k,m}} \quad \frac{1}{2} \sum_{k=1}^{Z_S} \sum_{m=1}^{Z_S} t_{k,m} \min\left\{\log\left(1 + H_k^{SR} p_k^S\right) \log\left(1 + H_m^{RD} p_m^R\right)\right\} \tag{5a}$$

$$\text{s.t.} \quad p_k^S, p_m^R \ge 0 \; \forall k \in \{1, \ldots, Z_S\}, m \in \{0, \ldots, Z_S\} \tag{5b}$$

$$\sum_{k=1}^{Z_S} p_k^S \Omega_k^{S,l} \le I_{th} \; \forall l \in \{1, \ldots, Z_P\} \tag{5c}$$

$$\sum_{m=1}^{Z_S} p_m^R \Omega_m^{R,l} \le I_{th} \; \forall l \in \{1, \ldots, Z_P\} \tag{5d}$$

$$\sum_{k=1}^{Z_S} p_k^S \le P_S, \; \sum_{m=1}^{Z_S} p_m^R \le P_R \tag{5e}$$

$$\sum_{k=1}^{Z_S} t_{k,m} = 1 \; \forall m; \; \sum_{m=1}^{Z_S} t_{k,m} = 1 \; \forall k \tag{5f}$$

$$t_{k,m} \in \{0, 1\} \quad \forall (k, m) \tag{5g}$$

where our target function in (5a) is the sum rate of all subcarrier pairs used by the SU and the relay from (3); constraints (5c) and (5d) ensure that the interference introduced to the PU in (4) is managed below a specified threshold I_{th}; constraint (5e) corresponds to the total power that can be used for the SU and the relay, respectively; and constraints (5f) and (5g) imply that each subcarrier of the SU and the relay can only be used once.

III. Heterogeneous Genetic Algorithm for Joint Subcarrier Pairing and Power Allocation

The problem in (5a)–(5g) is an MIP problem, where the indicator $t_{k,m} \in \{0, 1\}$ and the power allocation $p_{k,m}$'s for

subcarrier pairing (k, m) are positive real numbers, respectively. A straightforward solution for this MIP optimization problem is to conduct an exhaustive search by testing all $Z_S!$ possible subcarrier pairing (k, m) and then solve the corresponding power allocation $p_{k,m}$ for each pair. This approach, however, is infeasible for a practical number of subcarriers. The other methods, such as those in [15], [17], and [29], are based on imposing the following assumptions:

$$H_k^{SR} p_k^S = H_m^{RD} p_m^R \tag{6}$$

to simplify the target function in (5a) as

$$\frac{1}{2} \sum_{k=1}^{Z_S} \sum_{m=1}^{Z_S} t_{k,m} \log(1 + H_{k,m} p_{k,m}) \tag{7}$$

where, for a subcarrier pairing (k, m), the corresponding power allocation from the SU and the relay can be, respectively, expressed as

$$p_k^S = \frac{H_m^{RD}}{H_k^{SR} + H_m^{RD}} p_{k,m} \text{ and } p_m^R = \frac{H_k^{SR}}{H_k^{SR} + H_m^{RD}} p_{k,m} \tag{8}$$

with $p_{k,m} = p_k^S + p_m^R$. However, this approach may be suboptimal particularly when our problem has new interference management constraints (5c) and (5d). For example, if only subcarrier k of the source is overlapped with the PU bands, one should consider the source-to-PU channel to allocate p_k^S, but such a consideration is not necessary for allocating p_m^R. This implies that the approaches previously addressed in [15], [17], and [29] are only suboptimal in CR as the objective function is not the true target rate function given in (5a).[2]

To resolve the two aforementioned drawbacks for pure convex optimization methods, i.e., the extra assumption (6) and the integer constraints (5g), we adopt the GA framework. Although the GA cannot be guaranteed to reach the global optimal, these two drawbacks have less impact for the GA framework. A new HGA framework, which is a variant of the traditional GA [20], is adopted. The HGA can search for the true target rate function (5a) without simplification by (6). Moreover, the ingeniously devised chromosomes enable the HGA to handle subcarrier pairing and power allocation at the same time. Moreover, a good choice of initial conditions will render the HGA to converge more likely to good solutions. In our HGA, a chromosome is comprised of an integer string of length $2Z_s$ for subcarrier pairing and a positive real-number string of length $2Z_s$ for power allocation. The first and second halves of the $2Z_s$ genes, both of which are a permutation of $\{1, \ldots, Z_S\}$, are for the S–R and R–D links, respectively. The gene values corresponding to the kth subcarrier for the S–R link and the mth subcarrier for the R–D link are denoted by $SR(k)$ and $RD(m)$, respectively. If the kth subcarrier for the S–R link is paired with the mth subcarrier for the R–D link, then $SR(k) = RD(m)$, and $t_{k,m} = 1$.

[2]Note that in [29], the sum-rate upper bounds in [29, eq. (8)] were also based on the simplified rate (7) instead of the true target rate function (5a) (assumptions (6) or [29, eq. (6)] were imposed), and thus, the close-to-optimal claim was not valid.

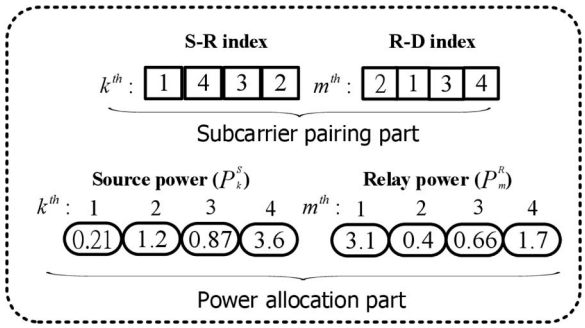

Fig. 2. Structure of the chromosome of our HGA, where p_k^S and p_m^R are the power allocation on the SR channel of the kth subcarrier and the RD channel of the mth subcarrier, respectively.

Furthermore, the power allocation part of each chromosome is divided into power allocation for the SU and power allocation for the relay, each of which is further divided into two parts according to whether the corresponding subcarriers are overlapped with the PU band or not. This is due to the fact that the gene values of the former are, in general, much smaller than those of the latter with the limitation of the interference to the PU. An example chromosome with the number of subcarriers $Z_S = 4$ is shown in Fig. 2, where the first $(k = 1)$ subcarrier of the SU is paired with the second subcarrier $(m = 2)$ of the relay. Our HGA is sketched as follows. We begin with the initialization with proper chromosomes, after progress such as evaluation, crossover, and mutation, and finally, a close-to-optimal chromosome (subcarrier pairing and power allocation) maximizing the fitness value (5a) will be found. The detailed steps are described in the following sections. We discuss the two initializations in Section III-A and the overall HGA in Section III-B. Finally, the convergence issue of our HGA is discussed in Section III-C.

A. *Initializations for the Subcarrier Pairing and Power Allocation for the HGA*

It is known that the performance of GAs heavily depends on the initialization of chromosomes. Typically, the randomly chosen chromosomes are used for initialization [20]. This initialization, however, in many cases, cannot result in satisfactory performance for the GAs. Motivated by [15], [19], and [29], we thus propose two new initialization methods, inspired by the convex optimization theory, for our HGA. The first initialization scheme can be treated as an extension of the Lagrangian dual methods in [15] and [29] with multiple CR constraints. Typically, the Lagrangian dual methods [15], [29] need a lot of subgradient iterations to reach convergence. In our first scheme, for each chromosome, less subgradient iterations are performed, as compared with [15] and [29]. However, since these subgradient iterations are performed for every chromomere, the overall complexity can be high. To reduce complexity, our second initialization scheme only performs subgradient iterations to generate *one* baseline chromosome, based on which we select good randomly generated chromosomes by measuring norms of their KKT residues [19].

Now, we introduce our new initializations of the parent chromosomes. To invoke convex optimization techniques, we simplify our optimization problem by imposing (6) on (5a)–(5g). However, different from [15] and [29], assumption (6) is imposed only in the initialization step, and the rest of our HGA steps focus on the original problem (5a)–(5g) without simplification. The simplified (5a)–(5g) are

$$\max_{p_{k,m}\geq 0, t_{k,m}} \quad \frac{1}{2}\sum_{k=1}^{Z_S}\sum_{m=1}^{Z_S} t_{k,m}\log(1+H_{k,m}p_{k,m}) \tag{9a}$$

$$\text{s.t.} \quad \sum_{k=1}^{Z_S}\sum_{m=1}^{Z_S} t_{k,m}C_{k,m}^{S}p_{k,m}\Omega_k^{S,l} \leq I_{th}$$

$$\forall l \in \{1,\ldots,Z_P\} \tag{9b}$$

$$\sum_{k=1}^{Z_S}\sum_{m=1}^{Z_S} t_{k,m}C_{k,m}^{R}p_{k,m}\Omega_m^{R,l} \leq I_{th}$$

$$\forall l \in \{1,\ldots,Z_P\} \tag{9c}$$

$$\sum_{k=1}^{Z_S}\sum_{m=1}^{Z_S} t_{k,m}C_{k,m}^{S}p_{k,m} \leq P_S$$

$$\sum_{k=1}^{Z_S}\sum_{m=1}^{Z_S} t_{k,m}C_{k,m}^{R}p_{k,m} \leq P_R \tag{9d}$$

$$\sum_{k=1}^{Z_S} t_{k,m} = 1,\ \forall m,\ \sum_{m=1}^{Z_S} t_{k,m} = 1\ \forall k \tag{9e}$$

$$t_{k,m} \in \{0,1\}\ \forall (k,m) \tag{9f}$$

where $H_{k,m} = H_k^{SR}H_m^{RD}/(H_k^{SR}+H_m^{RD})$ in (9a), whereas $C_{k,m}^{S} = H_m^{RD}/(H_k^{SR}+H_m^{RD})$ and $C_{k,m}^{R} = H_m^{SR}/(H_k^{SR}+H_m^{RD})$ in (9b) and (9c), respectively. The resulting two new initializations are delineated as follows. Note that the first initialization method also serves as the basis for the second initialization method.

1) Initializations Based on Solving Lagrange Dual Problems: In the first initialization method, we focus on the convex Lagrange dual problem of (9a)–(9f), which is much easier to solve, and new Lagrange dual variables will be assigned to each constraint in (9d)–(9f) correspondingly. We then iteratively solve the Lagrange dual variables and the original power allocation $p_{k,m}$'s. Given Lagrange dual variables, the power allocation is solved via waterfilling, whereas given power allocation, the dual variables can be found with subgradient methods [26]. After the iterations, the subcarrier pairing is solved following the methods in [15]. The resulting power allocation and subcarrier pairing are then used to form parent chromosomes. These steps are summarized in Table I(a).

First, we form the Lagrangian dual problem of (9a)–(9f). Note that different from the works in [15], [18], and [29], our dual problem takes into consideration multiple CR constraints. From (9a)–(9d), the Lagrangian $L(p_{k,m}, t_{k,m}, \beta_S, \beta_R, \gamma_{S_l}, \gamma_{R_l})$ is

$$\begin{aligned}
&\frac{1}{2}\sum_{k=1}^{Z_S}\sum_{m=1}^{Z_S} t_{k,m}\log(1+H_{k,m}p_{k,m}) \\
&+\beta_S\left(P_S - \sum_{k=1}^{Z_S}\sum_{m=1}^{Z_S} t_{k,m}C_{k,m}^{S}p_{k,m}\right) \\
&+\beta_R\left(P_R - \sum_{k=1}^{Z_S}\sum_{m=1}^{Z_S} t_{k,m}C_{k,m}^{S}p_{k,m}\right) \\
&+\sum_{l=1}^{Z_P}\gamma_{S_l}\left(I_{th} - \sum_{k=1}^{Z_S}\sum_{m=1}^{Z_S} t_{k,m}C_{k,m}^{S}p_{k,m}\Omega_k^{S,l}\right) \\
&+\sum_{l=1}^{Z_P}\gamma_{R_l}\left(I_{th} - \sum_{k=1}^{Z_S}\sum_{m=1}^{Z_S} t_{k,m}C_{k,m}^{R}p_{k,m}\Omega_m^{R,l}\right)
\end{aligned} \tag{10}$$

where γ_{S_l}, γ_{R_l}, β_S, and β_R are the dual variables corresponding to constraints (9b) and (9c), the first equation in (9d), and the

TABLE I
INITIALIZATION METHODS FROM CONVEX OPTIMIZATION FOR THE HGA IN TABLE II

(a) Initialization based on solutions of Lagrange dual problems

For (parent chromosome index $j=1$ to population size P_1)
  Randomly initialize dual variables $\beta_S^{(0)}, \beta_R^{(0)}, \gamma_{S_l}^{(0)}, \gamma_{R_l}^{(0)}$
  For (subgradient iteration $i=1$ to I_1)
    For all subcarrier pair (k,m)s, compute the power allocation $P_{k,m}^{(i)}$ using waterfilling in (12) via $\beta_S^{(i-1)}, \beta_R^{(i-1)}, \gamma_{S_l}^{(i-1)}, \gamma_{R_l}^{(i-1)}$.
    Compute dual variables $\beta_S^{(i)}, \beta_R^{(i)}, \gamma_{S_l}^{(i)}, \gamma_{R_l}^{(i)}$ using subgradient method in (13) via $\beta_S^{(i-1)}, \beta_R^{(i-1)}, \gamma_{S_l}^{(i-1)}, \gamma_{R_l}^{(i-1)}$, subcarrier pairing indicator $t_{k,m}$ and $P_{k,m}^{(i)}$.
  End
  Set the power allocation of the j^{th} parent chromosome $P_{k,m}^{*}$ as $P_{k,m}^{(I)}, \forall (k,m)$.
  Set the subcarrier pairing of the j^{th} parent chromosome $t_{k,m}^{*}$ from $P_{k,m}^{*}$ as [15].
End

(b) Initialization based on KKT residue

For parent chromosome index $j=1$, generate a baseline parent chromosome using methods in Table I-(a).
Compute the baseline KKT residue $\|\mathbf{r}\|_2^b$ for the baseline parent chromosome (index $j=1$) using (15)-(19).
While (index of parent chromosome $j <$ population size P_2)
  Generate random power allocation $P_{k,m}$.
  Compute the corresponding KKT residue $\|\mathbf{r}\|_2$ using $P_{k,m}$ and $t_{k,m}$ from (15)-(19).
  If KKT residue $\|\mathbf{r}\|_2 <$ baseline $\|\mathbf{r}\|_2^b/C$
    Accept the current random parent chromosome.
    Index of parent chromosome $j = j+1$.
  End
End

second equation in (9d), respectively. Moreover, from (10), the dual problem of (9a)–(9f) is

$$\min_{\beta_S,\beta_R,\gamma_{S_l},\gamma_{R_l}} \max_{p_{k,m}\geq 0, t_{k,m}} \quad L(p_{k,m}, t_{k,m}, \beta_S, \beta_R, \gamma_{S_l}, \gamma_{R_l})$$

$$\text{s.t.} \quad \sum_{k=1}^{Z_S} t_{k,m} = 1 \ \forall m; \ \sum_{m=1}^{Z_S} t_{k,m} = 1 \ \forall k$$

$$t_{k,m} \in \{0,1\} \ \forall k,m; \beta_S, \beta_R, \gamma_{S_l}, \gamma_{R_l} \geq 0. \tag{11}$$

Now, we show, given subcarrier pairing $t_{k,m}$, how to iteratively solve the corresponding optimal power allocation $p_{k,m}$ and dual variables $\beta_S, \beta_R, \gamma_{S_l}, \gamma_{R_l}$ in (11). With fixed $t_{k,m}$, the corresponding optimal power allocation is (12), shown at the bottom of the page, where $x^+ = \max\{0, x\}$. Note that (12) reflects that one should not allocate power $p_{k,m}$ for subcarrier pairing (k,m) if $C^S_{k,m}\sum_{l=1}^{Z_p}\Omega^{S,l}_k$ and $C^R_{k,m}\sum_{l=1}^{Z_p}\Omega^{R,l}_m$ are too large compared with $H_{k,m}$. This situation corresponds to the case where any nonzero $P_{k,m}$ will cause too much interference to the PU [see (9b) and (9c)] compared with the rate gain [see (9a)] it obtained. Now, for fixed $t_{k,m}$ and $p_{k,m}$, to update the dual variables β_S, β_R, γ_{S_l}, and γ_{R_l}, the subgradient method [26], [27] is used. Take γ_{S_l} as an example, from the constraint of interference to the PU (9b), the new value is updated from the old γ_{S_l} by

$$\gamma_{S_l} - \delta\left(I_{\text{th}} - \sum_{k=1}^{Z_S}\sum_{m=1}^{Z_S} t_{k,m}C^S_{k,m}p_{k,m}\Omega^{S,l}_m\right) \tag{13}$$

where δ is the step size. The other dual variables γ_{R_l}, β_S, and β_R are updated similarly from the dual variables corresponding to constraints (9c) and the first and second equations in (9d), respectively.

After iteratively solving power allocation $p_{k,m}$ and dual variables using (12) and (13), we then update the subcarrier pairings $t_{k,m}$ following the methods in [15]. Finally, to initialize other chromosomes, we generate new initial dual variables and subcarrier pairing and repeat the aforementioned procedure.

2) Initializations Based on KKT Residues: The main drawback of the previous initialization method is high complexity, because we need to perform iterations between power allocation and dual variables (12) and (13) for every parent chromosome. Thus, here, we propose another initialization scheme with complexity lower than that of the previous scheme. First, we only run a few iterations among power allocation and dual variables (12) and (13) for a baseline parent chromosome. We name the resulting dual variables for this baseline chromosome as $\gamma^b_{S_l}$, $\gamma^b_{R_l}$, β^b_S, and β^b_R. As for the rest of the parent chromosomes, we randomly generate the power allocation and subcarrier pairing but select the good ones by the KKT residues [19] using $\gamma^b_{S_l}, \gamma^b_{R_l}, \beta^b_S, \beta^b_R$. The KKT residue is a measure of the distance between a solution and the KKT solution (the solution satisfies the KKT conditions that are necessary for optimality [19]), and only the parent chromosomes with power allocation and subcarrier pairing close to the KKT solutions of (9a)–(9d) are selected. The steps are summarized in Table I(b).

To find the KKT residue of a parent chromosome, from the KKT condition for (9a)–(9d) given $t_{k,m}$, we can define the following residues:

$$r_1 = t_{k,m}\left[\frac{H_{k,m}}{2(1+H_{k,m}p_{k,m})} - C^S_{k,m}\left(\beta_S + \sum_{l=1}^{Z_p}\gamma_{S_l}\Omega^{S,l}_k\right)\right. \tag{14}$$

$$\left. - C^R_{k,m}\left(\beta_R + \sum_{l=1}^{Z_p}\gamma_{R_l}\Omega^{R,l}_m\right)\right] \tag{15}$$

$$r^l_2 = \sum_{l=1}^{Z_P}\gamma_{S_l}\left(I_{th} - \sum_{k=1}^{Z_S}\sum_{m=1}^{Z_S} t_{k,m}C^S_{k,m}p_{k,m}\Omega^{S,l}_k\right) \tag{16}$$

$$r^l_3 = \sum_{l=1}^{Z_P}\gamma_{R_l}\left(I_{th} - \sum_{k=1}^{Z_S}\sum_{m=1}^{Z_S} t_{k,m}C^R_{k,m}p_{k,m}\Omega^{R,l}_m\right) \tag{17}$$

$$r_4 = \beta_S\left(P_S - \sum_{k=1}^{Z_S}\sum_{m=1}^{Z_S} t_{k,m}C^S_{k,m}p_{k,m}\right) \tag{18}$$

$$r_5 = \beta_R\left(P_R - \sum_{k=1}^{Z_S}\sum_{m=1}^{Z_S} t_{k,m}C^S_{k,m}p_{k,m}\right) \tag{19}$$

$$\beta_S, \beta_R, \gamma_{S_l}, \gamma_{R_l} \geq 0, \quad l = 1, \ldots, Z_P. \tag{20}$$

If the subcarrier pairing $t_{k,m}$'s, power allocation $p_{k,m}$'s, and dual variables form the KKT solution, then all the residues in (15)–(19) are equal to zero. We define the KKT residue $\|\mathbf{r}\|^b_2$ as the summation of the squares of residues in (15)–(19), with dual variables set to $\gamma^b_{S_l}$, $\gamma^b_{R_l}$, β^b_S, and β^b_R. We then compare the KKT residue of the randomly generated parent chromosome with that of the baseline parent chromosome. The randomly generated parent chromosome is accepted only when its KKT residue is sufficiently small. For the power allocation part of a parent chromosome, it must satisfy the interference constraints (9b) and (9c) for the PU. To do this, we generate K random numbers between $\{0, \min(I_{\text{th}}/C^S_{k,m}\Omega^{S,l}_k, I_{\text{th}}/C^R_{k,m}\Omega^{R,l}_k)\}$, where K is the number of the subcarriers overlapped with the PU band, and choose the minimum among them as $P_{k,m}$. Next, we generate $Z_s - K$ random numbers between $(0, P_S + P_R)$ on those subcarriers nonoverlapped with the PU band. These randomly generated parent chromosomes are then selected according to the KKT residue $\|\mathbf{r}\|^b_2$ from (15)–(19).

$$p_{k,m} = \left[\frac{1}{2\left(C^S_{k,m}\left(\beta_S + \sum_{l=1}^{Z_p}\gamma_{S_l}\Omega^{S,l}_k\right) + C^R_{k,m}\left(\beta_R + \sum_{l=1}^{Z_p}\gamma_{R_l}\Omega^{Rl}_m\right)\right)} - \frac{1}{H_{k,m}}\right]^+ \tag{12}$$

TABLE II
HGA FOR SOLVING JOINT SUBCARRIER PAIRING AND POWER ALLOCATION (5A)–(5G)

Initialization: Generate parent chromosomes using Table I-(a) or Table I-(b)
For (generation index $g = 1$ to G_1 (G_2))
Step 1: Evaluation
Compute fitness values for current chromosomes using (5a).
Step 2: Truncated selection
Retains T chromosomes with higher fitness values, and then randomly select two of them for mating.
Step 3: Crossover operation
For the subcarrier pairing part, use the priority-based crossover in Fig 3.
For the power allocation part, use the arithmetic crossover $(1-\beta)\times p_a^S+\beta\times P_b^S$ in (21).
Step 4: Mutation operation
The power allocation parts are mutated by $LB_i+(UB_i-LB_i)\beta$ in (22) and the subcarrier pairing parts are mutated by the integer mutation.
Step 5: *Élitism*
If necessary, put the best chromosome in generation $g-1$ into current population to ensure *élitist* in Definition 1.
End
Find the chromosome within the population with maximum (5a) and return the corresponding $(P_k^S, P_m^R, t_{k,m})$.

B. Overall HGA

We summarize our HGA algorithms in Table II for solving (5a)–(5g). Apart from the new initialization step described in the previous section, here, we also propose new crossover and mutation steps in the HGA. For the crossover, we propose two different procedures to pass "good" genes from the parent chromosomes to the offsprings for the subcarrier pairing and power allocation parts, respectively. For the subcarrier pairing parts, the crossover with channel link strength as priority is proposed. For the power allocation parts, the arithmetic crossover is adopted. Next, we describe the detailed steps of our HGA in which every possible solution (subcarrier pairing and power allocation) is represented by a chromosome, as shown in Fig. 2.

Step 1—Evaluation: After initializations, the initial p_k^S and p_m^R in (5a) are obtained from (8). Then, the fitness values are computed for each of the P_1 (or P_2) parent chromosomes of the current population by substituting the corresponding subcarrier pairing index $t_{k,m}$ and power allocation p_k^S and p_m^R into the *original* target function (5a) [without simplification by (6)]. Here, P_1 and P_2 are the numbers of populations in the HGA in Table II with initialization in Table I(a) and (b), respectively. Note that the power allocation p_k^S's and p_m^R's are normalized to ensure that constraints (5b)–(5e) are satisfied.

Step 2—Selection: To preserve good chromosomes (solutions) to yield better offsprings, we employ the truncated selection scheme [20], which only retains T_1 ($T_1 < P_1$) or T_2 ($T_2 < P_2$) parent chromosomes that have larger fitness values. We then reproduce them in a mating pool and randomly select two parent chromosomes for the following crossover step.

Step 3—Crossover: Here, we will use two different crossover methods for the subcarrier pairing and power allocation parts for our chromosomes, as shown in Figs. 3 and 4, respectively. Our crossover method for the subcarrier pairing is based on an extension of the priority-based crossover in [32], and that for the power allocation part is based on the arithmetic crossover [23]. The details are described as follows.

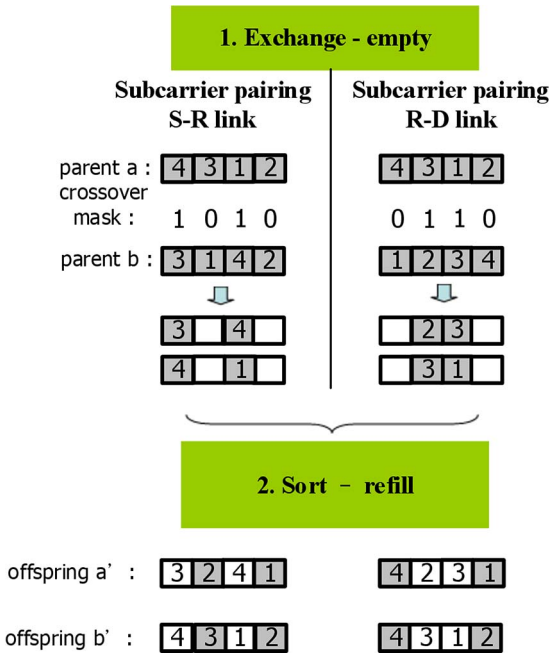

Fig. 3. Priority-based crossover for the subcarrier pairing, where $H_2^{SR} > H_4^{SR}$, and $H_1^{RD} > H_4^{RD}$.

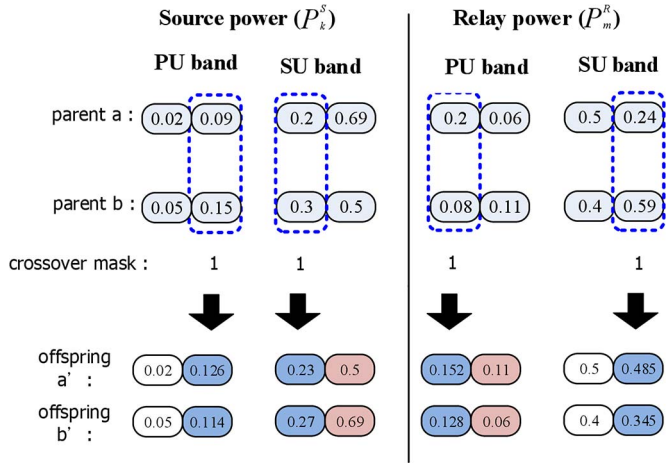

Fig. 4. Arithmetic crossover for the power allocation to reduce the interference to the PU, where the power allocation of the offsprings is the convex combination of those of the parent chromosomes.

The key idea for the priority-based crossover is to give "bad" genes lower priority in the chromosomes after crossover, which simply reflects the fitness-survival principle of the GA [20]. The priority is determined by the channel link strengths—the larger the channel link strength, the larger the gene value, and the higher the priority. The details are shown as follows, with an example shown in Fig. 3. In our priority-based crossover, we first construct a $2Z_S$-element crossover mask sequence that consists of 1's and 0's generated with equal probability [20], and then, we perform the exchange empty step. When the elements in the crossover mask are 1's, the genes of the two parent chromosomes in the corresponding positions will be

exchanged, whereas if they are 0's, the genes will be emptied. Next, in the sort-refill step, we will first sort the rest of the gene values and then refill the missing gene values sequentially according to the channel link strengths. For example, in Fig. 3, the values of the second and fourth genes are missing in the S–R link part of the offspring a'. Suppose that $H_2^{SR} > H_4^{SR}$, we thus fill in gene values 2 and 1 as the second and fourth genes in the S–R link part of the offspring chromosomes a', respectively. Likewise, we fill in gene values 3 and 2 as the second and fourth genes in the S–R link part of the offspring chromosomes b'. It is noteworthy that based on this crossover method, each gene combination of the subcarrier pairing part for the S–R and R–D links will always be a permutation of $\{1, \ldots, Z_S\}$. Then, the resulting subcarrier pairing for the offsprings is valid. We adopt the following simple observation for the aforementioned subcarrier pairing strategy, i.e., subcarriers with the same gene values in the S–R and R–D links are paired together. From our original target function in (5a), it is clear that without power allocation $p_k^S = p_m^R$, if $H_k^{SR} > H_m^{RD}$, the DF rate $\min\{\log(1 + H_k^{SR} p_k^S), \log(1 + H_m^{RD} p_m^R)\} = \log(1 + H_m^{RD} p_m^R)$. Thus, the rate is limited by the weaker link between the SU to the relay and the relay to the destination links. Thus, a bad subcarrier pairing may happen when a large H_k^{SR} is paired with a small H_m^{RD}, and *vice versa*. This observation, similar to that in [12], forms the basis of our subcarrier pairing part of the chromosomes and the proposed priority-based crossover.

The crossover operation in the power allocation part is based on the arithmetic crossover operation [23], as shown in Fig. 4. First, we create a four-element mutation mask sequence comprising 1's and 0's generated with equal probability, each of which is for the subcarriers either overlapped with the PU band or not for both the SU and the relay. If the corresponding element in the cross mask is equal to 1, the genes on the left side of the randomly picked mating point remain the same, the gene values on the right side of this point will be swapped, and the gene values of the offspring at the cross point will be a convex combination of those of the parent chromosomes, which are given by

$$p_{a'}^S = (1-\beta) \times p_a^S + \beta \times P_b^S \text{ and } p_{b'}^S = \beta \times p_a^S + (1-\beta) \times p_b^S \tag{21}$$

where p_a^S and p_b^S and $p_{a'}^S$ and $p_{b'}^S$ are the corresponding gene values (power allocation) of the two parent chromosomes and the offspring chromosomes, respectively, and β is randomly distributed in (0,1).

Note that if a subcarrier overlaps the PU band, the power allocated to it should be low. When p_a^S and p_b^S are small due to the limitation on the interference to the PU, the convex combination of the gene values ensures that the power allocation of the offspring, i.e., $p_{a'}^S$ and $p_{b'}^S$, will be small after the crossover for those subcarriers overlapped with the PU band. On the other hand, if a subcarrier of the SU is not in the PU band, then p_a^S and p_b^S can be large, and the resulting $p_{a'}^S$ and $p_{b'}^S$ will also be large. The arithmetic crossover then automatically passes the "good" genes (power allocation) to coexist with the PU from the parent chromosomes to the offsprings.

Step 4—Mutation: Our mutation operation is also divided into two parts: the uniform mutation for the power allocation part and the integer mutation for the subcarrier pairing part. We discuss the mutation for the power allocation part first. Here, we use the power allocation for the SU in Fig. 5 as an example. First, we divide the power allocation into two parts depending on whether the corresponding subcarriers are overlapped with the PU band or not. We then randomly generate a four-element mutation mask sequence comprising 1's and 0's generated according to the mutation probability p_m $(0 < p_m < 1)$ [20], each of which is for the subcarriers either overlapped with the PU band or not for both the S–R and R–D links. If the element of the mutation mask is 1, then we will randomly choose a gene (power allocation) to mutate. The corresponding power allocation in the offspring will become

$$LB_i + (UB_i - LB_i)\beta, \quad i = 1, 2 \tag{22}$$

where LB_i and UB_i denote the lower and upper bounds of the resulting power allocation values, respectively, and β is randomly distributed in (0, 1). If the subcarrier corresponds to the power allocation (genes) overlapped with the PU band, then $i = 1$; otherwise, $i = 2$. We choose $LB_1 < UB_1 < LB_2 < UB_2$ to reduce the interference to the PU. If the element of the mutation mask is 0, then the power allocation (genes) is left unchanged.

The integer mutation for the subcarrier pairing part works as follows. Similar to what has been discussed, we first generate a two-element mutation mask sequence, one of which is for the subcarriers in the S–R link and the other is for those in the R–D link. These two elements are either 1 or 0, generated with equal probability. If the element of the mask is 1, then the values of the two randomly selected genes are swapped. Otherwise, the gene values are left unchanged. An example is given in Fig. 5, where the two randomly selected gene values, e.g., the second

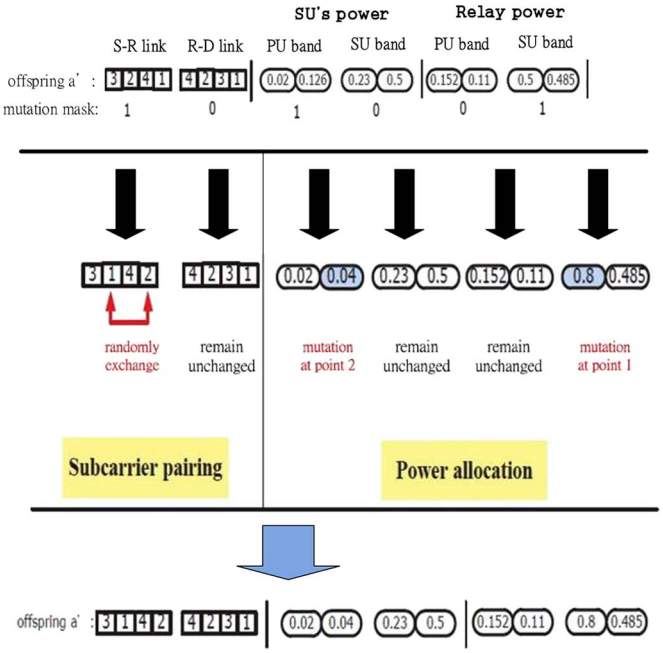

Fig. 5. Mutation operations of our HGA, where power allocation is mutated by (22), and subcarrier pairing is mutated by the integer mutation.

and fourth genes, in the S–R link part are swapped, and those in the R–D link part are left unchanged.

Step 5—Élitism: If the fitness values from (5a) of all chromosomes are smaller than the maximum value in the previous iteration, then we will replace the chromosome with the smallest fitness value with the best value in the previous iteration. The goal of this step is to ensure that the fitness values will be a nondecreasing sequence, which leads to the convergence of our HGA, as will be discussed in the following section. After the iterations are over, the chromosome with the maximum fitness value [target function in (5a)] is then chosen as our solution.

Our HGA will repeat the aforementioned Steps 1–5 until the number of the generation exceeds the limit.

C. Convergence Analysis

To scrutinize the convergence issue of our HGA, we first note the following definition from [22].

Definition 1: Any GA is said to be *élitist* if the following conditions hold for all generations.

Let $\mathbf{x}_g$ be the best chromosome at generation g. Then, at generation $g+1$, either

1) $\mathbf{x}_g$ is in the population, or
2) some chromosomes better than $\mathbf{x}_g$ are in the population.

For the *élitist* GA, we have the following theorem for convergence.

Theorem 1: Let $\mathfrak{X}_g$ be the population at generation g and $f(\mathfrak{X}_g)$ be the fitness value of the best chromosome in $\mathfrak{X}_g$ [33]. If the GA has mutation probability $0 < p_m < 1$, arbitrary crossover and selection, but is *élitist*, then the sequence

$$f^* - f(\mathfrak{X}_g)$$

where f^* is the optimal fitness value, is a nonnegative supermartingale that converges almost surely to zero.

Here, by definition [22], the random distance sequence $f^* - f(\mathfrak{X}_g)$ is a supermartingale, if the expected distance corresponding to generation $g+1$ is strictly smaller than the distance corresponding to current generation g, $\forall g$. For the HGA, we can readily note that it is *élitist* due to Step 5. It follows that the HGA with either initialization scheme will be ensured to converge based on the given theorem.

IV. Low-Complexity Two-Stage Algorithm With Separate Subcarrier Pairing and Power Allocation

Note that compared with the conventional GA with random initializations, our HGAs in Section III have higher complexity due to the new initializations in Table I and the lengthy chromosomes due to such joint consideration of subcarrier pairing and power allocation. To mitigate the computational overhead, here, we consider a two-stage approach that solves these two problems separately. Here, we propose to first use the GA with integer genes to determine the subcarrier pairing and then use another GA with real-number genes to solve the corresponding power allocation among the source and the relay. The steps are summarized in Table III and briefly discussed as follows.

TABLE III
Low-Complexity Two-Stage GA With Separate Subcarrier Pairing and Power Allocation

First stage : Subcarrier pairing using the GA with integer genes
Initialization: Generate parent chromosomes using methods in Table I-(b)
For (generation index $g = 1$ to G_4)
Step 1: Evaluation : Compute fitness values for current chromosomes using (5a) with $p_k^S = p_m^R, \forall k, m$.
Step 2: Truncated selection : same as Table II
Step 3: Crossover : priority-based crossover in Fig 3
Step 4: Mutation : Integer mutation
Step 5: *Élitism* : same as Table II
End
Find the chromosome within the population with the maximum (5a) and return corresponding $t_{k,m}$.
Second stage : Refine power allocation using the GA with real number genes
Initialization: Generate parent chromosomes using random p_k^S and p_m^R
For (generation index $g = 1$ to G_4)
Step 1: Evaluation : Compute fitness values for current chromosomes using (5a).
Step 2: Truncated selection : same as Table II
Step 3: Crossover : arithmetic crossover $(1-\beta) \times p_a^S + \beta \times P_b^S$ in (21)
Step 4: Mutation : using $LB_i + (UB_i - LB_i)\beta$ in (22)
Step 5: *Élitism* : same as Table II
Find the chromosome within the population with the maximum (5a) and return corresponding power allocation.

First Stage—Subcarrier Pairing Using GA With Integer Genes: The chromosome for the subcarrier pairing part is composed of $2Z_S$ genes, where the gene values for the S–R and R–D links are both permutations of $\{1, \ldots, Z_S\}$. The corresponding GA then begins with creating parent chromosomes using the initialization based on the KKT residue in Table I(b). However, different from the HGA in Section III, we use the uniform power allocation where $p_{k,m}$'s are equal for each subcarrier pairing (k, m). The rest of the steps in Table III, such as selection, crossover, mutation, and *élitist* steps, are similar to those in Section III-B, but only deal with the subcarrier pairing part. The aforementioned steps are then repeated until the number of generations exceeds the limit and after which the chromosome with the maximum fitness value (target function (5a) with equal power allocation) is chosen. The resulting subcarrier pairing is employed in the second stage. Note that the convergence of this step is ensured based on the discussion in Section III-C.

Second Stage—Refined Power Allocation Using GA With Real-Number Genes: In the second stage, after determining the subcarrier pairing $t_{k,m}$, we also use the GA with real-number genes to find the power allocation. Each chromosome consists of $2Z_s$-length genes corresponding to p_k^S and p_m^R, respectively. The rest of the steps in Table III, such as crossover and mutation, are similar to those in Section III-B, but only deal with the power allocation part.

A. Comparison of Complexity

We also compare the complexity of our algorithms in Table IV. The complexity of the HGA using the initialization in Table I(a) is mainly contributed by that of the initialization

TABLE IV
COMPARISON OF THE COMPLEXITY OF VARIOUS ALGORITHMS

Algorithms	Multiplications required
HGA in Table II with initialization in Table I-(a)	$O((Z_S{}^2I_1)P_1+G_1P_1Z_s)$
HGA in Table II with initialization in Table I-(b)	$O(Z_S{}^2I_1+G_2P_2Z_S)$
HGA in Table II with random initialization	$O(G_3P_3Z_S)$
Two-stage GA in Table III	$O(Z_S{}^2I_1+G_4P_4Z_s)$
Amendment algorithm [15]	$O(Z_S{}^2I_2)$
Hungarian method [16]	$O(Z_S{}^2I_2)$
SCP method [12]	$O(Z_S{}^2I_2)$
Exhaustive search	$O(Z_S!)$

step, which is $\mathcal{O}((Z_S^2I_1 + Z_S^3)P_1)$, whereas that of the rest is $\mathcal{O}(G_1P_1Z_S)$, where G_1 is the number of generations of the HGA using the initialization in Table I(a), Z_S is the total number of subcarriers, P_1 is the number of parent chromosomes (population size), and $I_1 \gg Z_s$ is the number of iterations required for the subgradient method for computing the dual variables in (13). As for the HGA with the initialization method in Table I(b), the main complexity of the initialization in generating the baseline parent chromosome and the overall complexity is $\mathcal{O}(Z_S^2I_1 + G_2P_2Z_S)$, where G_2 and P_2 are, respectively, the numbers of generations and of parent chromosomes (population size) of the HGA using the initialization in Table I(b). If our HGA in Table II uses a simple random initialization instead of those in Table I, the complexity will be $\mathcal{O}(G_3P_3Z_S)$, where G_3 and P_3 are, respectively, the numbers of generations and of population size. Although the complexity of our two-stage GA in Table III seems similar to that of the HGA using the initialization in Table I(b), the former can converge with smaller numbers of generations and of population size $(G_4P_4 < G_2P_2)$ and have less complexity.

We also list the complexity of algorithms in [12], [15], and [16] in Table IV, with I_2 being the corresponding number of iterations to converge. Note that our HGA in Table I(b) only run a few subgradient iterations (not until convergence) compared with [15] $(I_1 \ll I_2)$, and thus, the complexity will be much lower than that of [15]. As for the Hungarian [16] and SCP [12] methods in Table IV, the power allocations are found by waterfilling. Since the complexity of each algorithm heavily depends on the number of iterations in Table IV, we will provide a computer simulation using CPU time as a metric in the following section.

V. SIMULATIONS

Simulations are conducted in this section to compare the rate performance of our algorithms with previous works. In the considered OFDM-based cognitive relay networks as described in Section II-A, the channel coefficients h_k^{SR} and h_m^{RD} of the subcarriers for S–R and R–D links are drawn from independent and identically distributed Rician fading distributions with unit K-factor [11]. The variance of the additive noise N_0 is assumed to be unity. In the following, with slight abuse of notations, power constraints P_S, P_R and interference constraints $I_{\rm th}$ are replaced with P_S/N_0, P_R/N_0, and $I_{\rm th}/N_0$, respectively (and, thus, measured in decibels). The interferences to PUs are generated according to (4) with equivalent channel gains generated as in [13]. Without loss of generality, we assume that both

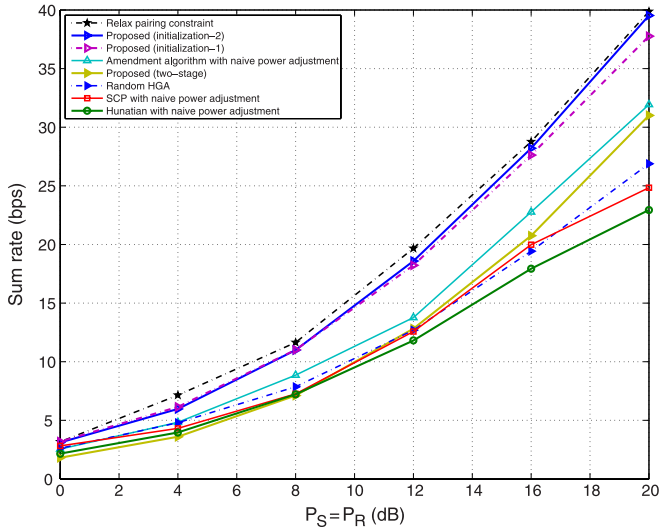

Fig. 6. Sum-rate comparison with the SU having $Z_S = 32$ subcarriers and $Z_P = 2$ PUs under interference management constraint $I_{\rm th} = -10$ dB.

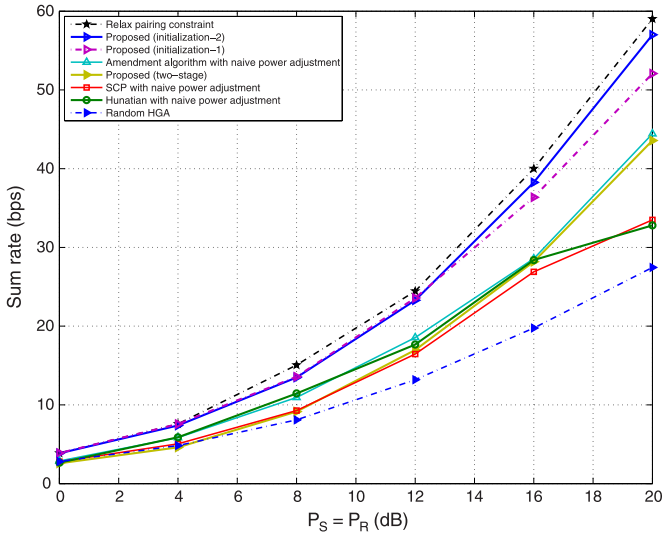

Fig. 7. Sum-rate comparison with the SU having $Z_S = 64$ subcarriers and $Z_P = 3$ PUs under interference management constraint $I_{\rm th} = -10$ dB.

the source and the relay have the same power constraints as $P_S = P_R$.

First, we compare the SU's sum rate over all subcarriers versus the transmitted power values P_s in Figs. 6 and 7. In Fig. 6, we use the number of subcarriers $Z_s = 32$ and the number of PUs $Z_p = 2$. The curves labeled as "relaxing pairing constraint" are obtained by removing the sum constraints of the subcarrier pairing $\sum_{k=1}^{Z_S} t_{k,m} = 1,\ \forall m$, $\sum_{m=1}^{Z_S} t_{k,m} = 1,\ \forall k$ in optimization problem (9a)–(9f). Thus, each source subcarrier can match with either more than one relay subcarrier or nothing. In Fig. 6, the HGA in Table II with the initialization in Table I(b) has the highest rate apart from the impractical "relaxing pairing constraint" curve. The HGA in Table II with the initialization in Table I(a) has performance next to the HGA in Table II with the initialization in Table I(b). Note that the SCP methods [12], the Amendment algorithm [15], and the Hungarian methods [16]

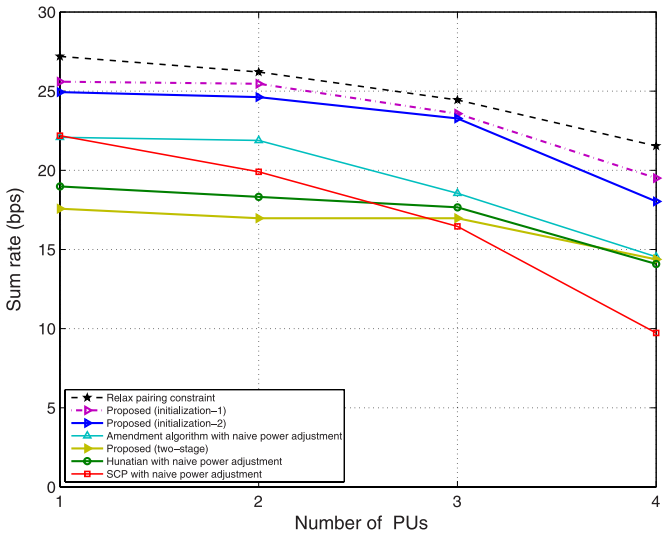

Fig. 8. Sum rate versus total number of PUs Z_p under interference management constraint $I_{\text{th}} = -10$ dB, with $Z_s = 64$ subcarriers and $P_S = P_R = 12$ dB.

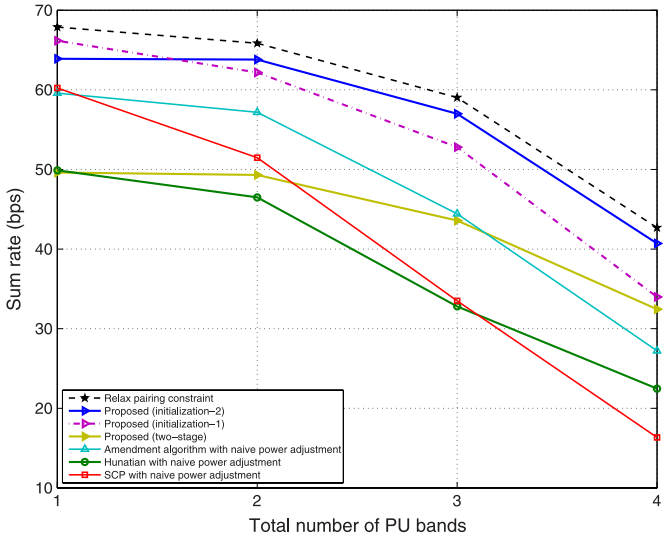

Fig. 9. Sum rate versus total number of PUs Z_p under interference management constraint $I_{\text{th}} = -10$ dB, with $Z_s = 64$ subcarriers and $P_S = P_R = 20$ dB.

are designed without considering the interference to the PU bands. In our simulations, they are combined with naive power allocations to deal with the interference constraints. That is, the power allocations were first found without considering the interference constraints. Then, power values corresponding to subcarriers overlapped with the PU were lowered to meet the interference constraint while the others are raised under the same total power over subcarriers. With naive power adjustments, these three algorithms from [12], [15], and [16] have lower rates compared with our two proposed algorithms aforementioned. As for the two-stage algorithm in Table III, it has comparable rate performance with the Amendment algorithm, but with much lower complexity, as shown in Table IV and Fig. 10. In Fig. 7, we use the number of subcarriers $Z_S = 64$ and the number of PUs $Z_P = 3$. Our HGA in Table II with the initialization in Table I(b) still has the best rate performance in this figure. Next, as in Fig. 7, the HGA in Table II with the initialization in Table I(b) [or Table I(a)] has higher rates than the algorithms from [12], [15], and [16]. The two-stage GA in Table III also has comparable rate performance with those of the algorithms in [12], [15], and [16]. In the end, the HGA with random initialization has the lowest rate, and it confirms that proper initialization is crucial for the HGA.

In Figs. 8 and 9, we consider the impact of different numbers of PUs Z_P on the rate performance, with the source/relay power being $P_S = P_R = 12$ dB and 20 dB, respectively. The number of subcarriers is 64, and the interference management constraint is $I_{\text{th}} = -10$ dB. In Fig. 8, we can see that our proposed algorithms in Table II outperform those in [12], [15], and [16], as shown in Figs. 6 and 7. Moreover, all algorithms have worse rates when the number of PUs Z_p increases. However, the rate of SCP with waterfilling [12] rapidly decreases because the corresponding subcarrier pairing method is too simple compared with the other algorithms. Similar observations can be found in Fig. 9. The HGAs in Table II always have better rates than the other algorithms [12], [15], [16]. According to Fig. 9, we can realize that the rates of all algorithms reduce with the rising number of PUs. Particularly when the number of the PUs $Z_P = 4$, the decrease in the sum rate is the most significant. This is because in our simulation settings, more PUs will result in larger interference to the SU and the relay, as well as more interference management constraints for the resource allocation.

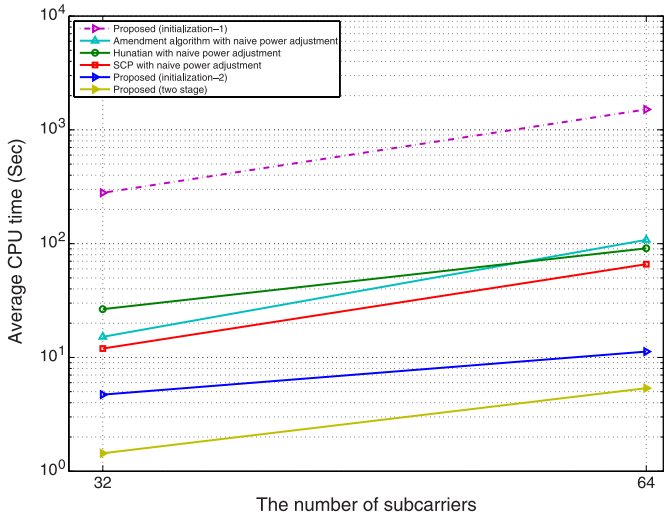

Fig. 10. Complexity comparison based on average CPU time.

Here, we also show the complexity of the proposed algorithms in Fig. 10 measured by CPU time. Compared with the complexity of the HGA using Table I(a) and that of the HGA using Table I(b), the latter has lower complexity since we only need to run subgradient iterations for the baseline chromosome. Moreover, our HGA with the initialization based on the KKT residue [see Table I(b)] can have lower complexity than the Lagrangian dual method (Amendment algorithm [15]), since we only run fewer subgradient iterations than the algorithm in [15] to get coarse dual variables. In Figs. 6 and 7, compared with the Lagrangian dual method (Amendment algorithm), the HGA with the initialization in Table I(b) has the sum-rate improvement of about 23.80% and 28.29% at

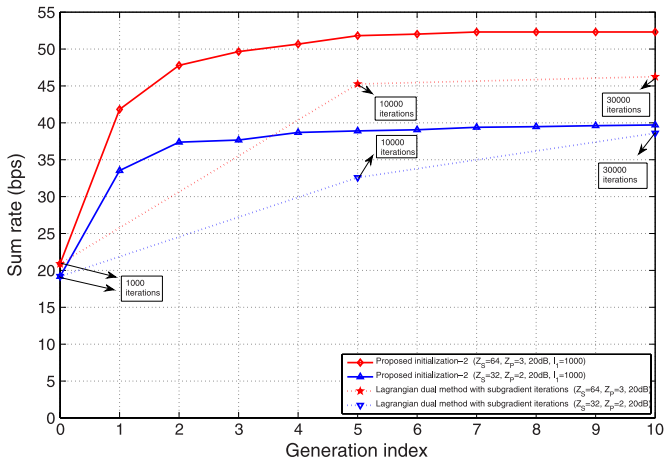

Fig. 11. Sum rate versus number of generations of the HGA initialization-2 [see Table II(b)]. Sum rates using the initialization in Table II(a) with sufficient iterations for convergence (30 000) are also shown for comparison.

20 dB. Thus, the benefit of the GA is that one can use less subgradient iterations in the Lagrangian dual method than those in the literature by refining the resource allocation using the GA framework (mutation and crossover). This observation is also verified in Fig. 11, which shows the sum rates over the generations of the HGA using the initialization in Table I(b). The rates with Generation Index 0 corresponds to the solution obtained from the Lagrangian dual method (with less (10^3) subgradient iterations). We can see that the rates are improved using the GA frameworks. Moreover, we also show the rate of the Lagrangian dual method with enough iterations $(3 * 10^4)$ to reach the convergence. When the number of PUs Z_p increases, our HGA has more gains compared with the Lagrangian dual method. The reasons are that assumptions (6) in the Lagrangian dual method limit the rate more when Z_p increases, whereas our HGA does not impose (6) after initializations.

VI. Conclusion

In this paper, we have considered the joint subcarrier pairing and power allocation problems for OFDM-based DF networks under interference management constraints for the PUs. We have proposed an HGA-based algorithm with two new initialization schemes inspired by the convex optimization theory and another two-stage GA-based algorithm to reduce complexity. The HGA framework can reduce the impact of extra assumptions made in previous works to apply convex optimization techniques. Conducted simulations show that our HGA with either initialization scheme provides superior performance compared with previous works and that our two-stage algorithm has competing performance with previous works while maintaining lower complexity.

References

[1] J. Mitola and G. Q. Maquire, Jr., "Cognitive radio: Making software radios more personal," *IEEE Pers. Commun.*, vol. 6, no. 4, pp. 13–18, Aug. 1999.

[2] E. Hossain and V. K. Bhargava, ed. *Cognitive Wireless Communication Networks*. New York, NY, USA: Springer-Verlag, 2007.

[3] T. Weiss and F. K. Jondral, "Spectrum pooling: An innovative strategy for the enhancement of spectrum efficiency," *IEEE Commun. Mag.*, vol. 42, no. 3, pp. S8–14, Mar. 2004.

[4] Y.-C. Liang, K.-C. Chen, G. Y. Li, and P. Mahonen, "Cognitive radio networking and communications: An overview," *IEEE Trans. Veh. Technol.*, vol. 60, no. 7, pp. 3386–3407, Sep. 2011.

[5] P.-H. Lin, S.-C. Lin, H.-J. Su, and Y.-W. P. Hong, "Improved transmission strategies for cognitive radio under the coexistence constraint," *IEEE Trans. Wireless Commun.*, vol. 11, no. 11, pp. 4058–4073, Nov. 2012.

[6] A. Sendonaris, E. Erkip, and B. Aazhang, "User cooperation diversity—Part I: System description," and "User cooperation diversity—Part II: Implementation aspects and performance analysis," *IEEE Trans. Commun.*, vol. 51, no. 11, pp. 1927–1938, Nov. 2003.

[7] J. Laneman, D. Tse, and G. Wornell, "Cooperative diversity in wireless networks: Efficient protocols and outage behavior," *IEEE Trans. Inf. Theory*, vol. 50, no. 12, pp. 3062–3080, Dec. 2004.

[8] K. Azarian and H. El Gamal, "On the achievable diversity–multiplexing tradeoff in half-duplex cooperative channels," *IEEE Trans. Inf. Theory*, vol. 51, no. 12, pp. 4152–4172, Dec. 2005.

[9] Y. Shen, S. Wang, and Z. Wei, "Joint subchannel pairing and power control for cognitive radio networks with amplify-and-forward relaying," *Sci. World J.*, vol. 2014, no. 8, Jun. 2014, Art. ID. 380106.

[10] M. O. Hasna and M.-S. Alouini, "Optimal power allocation for relayed transmission over Rayleigh-fading channels," *IEEE Trans. Wireless Commun.*, vol. 3, no. 6, pp. 1999–2004, Nov. 2004.

[11] D. Tse and P. Viswanath, *Fundamentals of Wireless Communication*. Cambridge, U.K.: Cambridge Univ. Press, 2005.

[12] Y. Li, W. Wang, J. Kong, and M. Peng, "Subcarrier pairing for amplify-and-forward and decode-and-forward OFDM relay links," *IEEE Commun. Lett.*, vol. 13, no. 4, pp. 209–211, Apr. 2009.

[13] G. Bansal, M. J. Hossain, V. K. Bhargava, and T. Le-Ngoc, "Subcarrier and power allocation for OFDMA-based cognitive radio systems with joint overlay and underlay spectrum access mechanism," *IEEE Trans. Veh. Technol.*, vol. 62, no. 3, pp. 1111–1122, Mar. 2013.

[14] G. A. S. Sidhu, F. Gao, W. Chen, and W. Wang, "Joint subcarrier pairing and power loading in relay aided cognitive radio networks," in *Proc. IEEE Wireless Commun. Netw. Conf.*, Apr. 2012, pp. 669–673.

[15] C.-N. Hsu, H.-J. Su, and P.-H. Lin, "Joint subcarrier pairing and power allocation for OFDM transmission with decode-and-forward relaying," *IEEE Trans. Signal Process.*, vol. 59, no. 1, pp. 399–414, Jan. 2011.

[16] X. Li, Q. Zhang, G. Zhang, and J. Qin, "Joint power allocation and subcarrier pairing for cooperative OFDM AF multi-relay networks," *IEEE Commun. Lett.*, vol. 17, no. 5, pp. 872–875, May 2013.

[17] T. Wang, Y. Fang, and L. Vandendorpe, "Power minimization for OFDM transmission with subcarrier-pair based opportunistic DF relaying," *IEEE Commun. Lett.*, vol. 17, no. 3, pp. 471–474, Mar. 2013.

[18] X. Zhang, X. Tao, Y. Li, N. Ge, and J. Lu, "On relay selection and subcarrier assignment for multiuser cooperative OFDMA networks with QoS guarantees," *IEEE Trans. Veh. Technol.*, vol. 63, no. 9, pp. 4704–4717, Nov. 2014.

[19] S. Boyd and L. Vandenberghe, *Convex Optimization*. Cambridge, U.K.: Cambridge Univ. Press, 2004.

[20] J. H. Holland, *Genetic Algorithms*. New York, NY, USA: Sci. Amer., 1992.

[21] K. Tank, K. Man, S. Kwong, and Q. He, "Genetic algorithm and their applications," *IEEE Signal Process. Mag.*, vol. 13, no. 6, pp. 22–37, Nov. 1996.

[22] C. R. Reeves and J. E. Rowe, *Genetic Algorithms—Principles and Perspectives*. Boston, MA, USA: Kluwer, 2003.

[23] T. Yalcinoz and H. Altum, "Power economic dispatch using a hybrid genetic algorithm," *IEEE Power Eng. Rev.*, vol. 21, no. 3, pp. 59/60, Mar. 2001.

[24] W. Yu and T. Lan, "Transmitter optimization for the multi-antenna downlink with per-antenna power constraints," *IEEE Trans. Signal Process.*, vol. 55, no. 6, pp. 2646–2660, Jun. 2007.

[25] H.-S. Lang, F.-T. Yeh, S.-C. Lin, and W.-H. Fang, "Joint subcarrier pairings and power allocations with interference management in cognitive relay networks based on genetic algorithms," in *Proc. Int. Conf. Intell. Green Building Smart Grid*, Taipei, Taiwan, Apr. 2014, pp. 1–5.

[26] S. Boyd and A. Mutapcic, "Subgradient methods," *Lecture Notes of EE364b*. Stanford, CA, USA: Stanford Univ., Spring quarter 2007/2008.

[27] W. Yu and R. Lui, "Dual methods for nonconvex spectrum optimization of multicarrier systems," *IEEE Trans. Commun.*, vol. 54, no. 7, pp. 1310–1322, Jul. 2006.

[28] H. W. Kuhn, "The Hungarian method for the assignment problem," in *50 Years of Integer Programming 1958–2008*. Berlin, Germany: Springer-Verlag, 2010, pp. 29–47.

[29] M. Shaat and F. Bader, "Asymptotically optimal subcarrier matching and power allocation for cognitive relays with power and interference constraints," in *Proc. IEEE Wireless Commun. Netw. Conf.*, Apr. 2012, pp. 663–668.
[30] Y. Liu and W. Chen, "Limited feedback based adaptive power allocation and subcarrier pairing for OFDM DF relay networks with diversity," *IEEE Trans. Veh. Technol.*, vol. 61, no. 6, pp. 2559–2571, Jul. 2012.
[31] Y. Liu and W. Chen, "Adaptive resource allocation for improved DF aided downlink multi-user OFDM systems," *IEEE Wireless Commun. Lett.*, vol. 1, no. 6, pp. 557–560, Dec. 2012.
[32] H.-Y. Lu and W.-H. Fang, "Joint receive antenna selection and symbol detection for MIMO systems: A heterogeneous genetic approach," *IEEE Commun. Lett.*, vol. 13, no. 2, pp. 97–99, Feb. 2009.
[33] G. Rudolph, *Convergence Properties of Evolutionary Algorithms*. Hamburg, Germany: Verlag, 1997.
[34] M. Grant and S. Boyd, CVX: Matlab Software for Disciplined Convex Programming, MathWorks, Inc., 2008.

Hung-Sheng Lang received the M.S. degree in electrical engineering from National Taiwan University of Science and Technology, Taipei, Taiwan, in 2013.

He is currently an Engineer with Foxconn, New Taipei City, Taiwan. His research interest includes data center solutions.

Shih-Chun Lin (M'08) received the B.S. and Ph.D. degrees in electrical engineering from National Taiwan University, Taipei, Taiwan, in 2000 and 2007, respectively.

In 2007, he was a Visiting Student with The Ohio State University, Columbus, OH, USA. After finishing his military duty in 2008, he became a Postdoctoral Researcher with National Tsing Hua University, Hsinchu, Taiwan. From August 2011 to August 2012, he was an Assistant Professor with National Taipei University of Technology, Taipei. He is currently an Assistant Professor with National Taiwan University of Science and Technology, Taipei. His research interests include coding/information theory, communications, and signal processing.

Dr. Lin received the Project for Excellent Junior Research Investigators from the Ministry of Science and Technology, Taiwan, in 2015 and was included in 2016 *Marquis Who's Who in the World*. He also served as a Track Chair for the 2014 International Conference on Intelligent Green Building and Smart Grid and as a Technical Program Committee Member for the IEEE International Conference on Communications (ICC), the ICC Workshop on Wireless Physical Layer Security, and the IEEE Vehicular Technology Conference (Spring).

Wen-Hsien Fang received the B.S. degree in electrical engineering from National Taiwan University, Taipei, Taiwan, in 1983 and the M.S.E. and Ph.D. degrees in electrical engineering and computer science from the University of Michigan, Ann Arbor, MI, USA, in 1988 and 1991, respectively.

In the Fall of 1991, he joined the faculty of National Taiwan University of Science and Technology, Taipei, where he is currently a Professor with the Department of Electronic and Computer Engineering. His research interests span various facets of signal processing applications, including statistical signal processing, signal processing for wireless communications, and multimedia signal processing.